JCTC Journal of Chemical Theory and Computation

Stabilities and Spin Distributions of Benzannulated Benzyl Radicals

Yongqiang Sui,[†] Rainer Glaser,*[,†] Ujjal Sarkar,[†] and Kent Gates[†,‡]

Departments of Chemistry and Biochemistry, University of Missouri—Columbia, Columbia, Missouri 65211

Received March 5, 2007

Abstract: The effects have been studied of mono- and dibenzannulation of a benzyl radical with hybrid density functional theory (B3LYP) and quadratic configuration interaction theory (QCISD). Bond dissociation energies and enthalpies are reported that were determined at the common level QCISD/6-311G**//B3LYP/6-31G* for the benzylic C−H bonds of toluene **1H**, the monobenzannulated polycyclic aromatic hydrocarbons (PAH) 1- and 2-methylnaphthalene **2H** and **3H**, the dibenzannulated PAHs 9-methylanthracene **4H** and 9-methylphenanthrene **5H**, and the model hydrocarbons 1-phenylpropene **6H** and propene **7H**. The conformational preferences and the symmetries of **1H**−**7H** and of their corresponding radicals **1**−**7** have been determined. The analysis of the electron and spin density distributions of radicals **1**−**7** at the QCI level are reported, and these high-level data are discussed in comparison to results obtained with density functional theory and with an awareness of a general perception shaped by Hückel molecular orbital theory. The results show in a compelling fashion that electron and spin delocalization onto an annulated arene is not the decisive principle for stabilization of the benzyl radicals formed by homolysis of the methylated PAHs $C_{10}H_7-CH_3$ and $C_{14}H_9-CH_3$, and instead, the analysis of QCI spin density distributions suggests that spin delocalization onto annulated arenes is avoided as much as possible while spin polarization does occur to a significant extent.

Introduction

The homolysis of toluene to yield a benzyl radical is discussed in many textbooks on organic chemistry as the prima facie example of the benefits of electron and spin delocalization (Chart 1). The hyperfine coupling in electron spin resonance (ESR) spectra shows that spin delocalization occurs, and quantum chemistry shows the spin delocalization to occur with some spin polarization (Figure 1). Dust and Arnold argued that increased spin delocalization should increase radical stability and proposed a relation between ESR hyperfine coupling constants and radical stabilization.[1] The textbook view on spin delocalization permeates the modern research literature,[2−5] and for example, Wu et al.[5] concluded from their studies of neutral para-substituted toluenes that "both electron-donating and electron-withdrawing groups reduce the bond dissociation energy (BDE) of the benzylic C−H bond [by 0−3 kcal/mol] because both groups cause spin delocalization from the benzylic radical center."

While restricted Hartree−Fock (HF) theory presents a good starting point for the computation of closed-shell molecules, studies of radicals are more challenging for a number of reasons.[6] Restricted and unrestricted open-shell HF (ROHF and UHF, respectively) theories[7,8] have been developed. While ROHF theory completely neglects spin polarization, UHF theory suffers from spin contamination (i.e., an overestimation of spin polarization). Spin contamination of the UHF solution can be remedied,[9,10] but spin polarization intrinsically is a correlation effect, and correlated methods are required to compute meaningful spin density distributions.[11−13] In practice, this is often accomplished by post-Hartree−Fock treatments[14] either with perturbation

* Corresponding author e-mail: glaserr@missouri.edu.
[†] Department of Chemistry.
[‡] Department of Biochemistry.

10.1021/ct700051j CCC: $37.00
Published on Web 04/20/2007

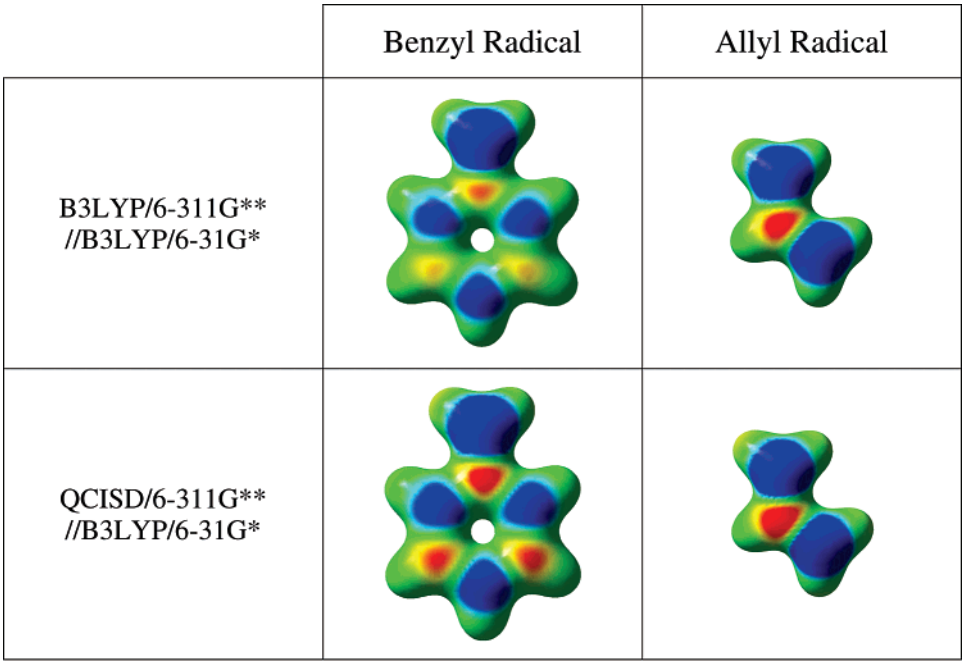

Figure 1. Spin density distributions of benzyl and allyl radicals color-coded (-4.432×10^{-3} to 4.432×10^{-3}) and displayed on isosurfaces of the electron densities (value 0.04).

Chart 1. Spin Delocalization in Benzyl Radical **1** and Its Dibenzannulated Derivative **4**

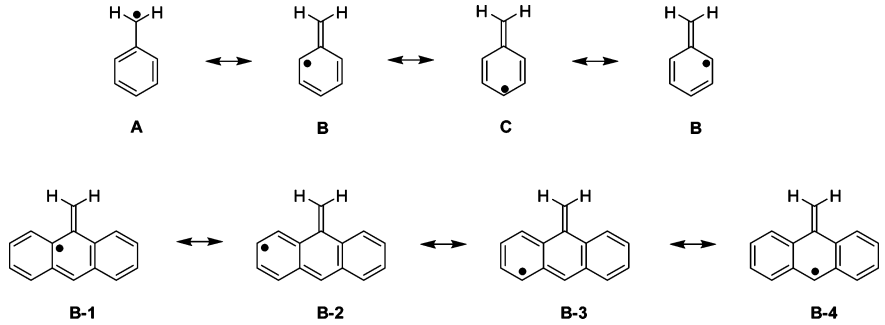

methods (i.e., Møller−Plesset perturbation theory[15]) or configuration interaction treatments (i.e., quadratic configuration interaction, QCI, theory[16]). Studies of radicals have become more frequent with the availability of density functional methods, and the usual spin contaminations are moderate.[17,18] This knowledge has been the implicit justification for the use of density functional theory (DFT) methods even though problems with spin-projected density functional theory are known.[19,20] Aside from the theoretical challenges, computations of radicals push the limits of computational feasibility because unrestricted theory doubles the number of orbitals and thereby greatly increases the post-HF task. Hence, accurate studies of benzene-sized radicals are scarce, higher-level studies of benzannulation effects of radicals have not been reported, and the conceptional knowledge about spin density distributions in benzannulated systems has not been well-developed.

In this article, we report the results of a theoretical study of benzannulation on the stabilities and the spin distributions of benzyl radical **1** and its benzannulated derivatives **2**−**5** (Chart 2). Allyl radicals **6** and **7** serve as models for **5**. Bond dissociation energies and enthalpies are reported that were determined at the common level QCISD/6-311G**//B3LYP/6-31G* for the benzylic C−H bonds of toluene **1H**, the monobenzannulated polycyclic aromatic hydrocarbons (PAHs) 1- and 2-methylnaphthalene **2H** and **3H**, the dibenzannulated PAHs 9-methylanthracene **4H** and 9-methylphenanthrene **5H**, and the model hydrocarbons 1-phenylpropene **6H** and propene **7H**. Conformational preferences and symmetries of **1H**−**7H** and **1**−**7** have been explored. Analyses of the electron and spin density distributions of radicals **1**−**7** have been performed at the DFT and QCI levels, and the results

Chart 2. Benzyl Radical **1**, Benzannulated Benzyl Radicals **2**−**5**, Model System **6**, and Allyl Radical **7**

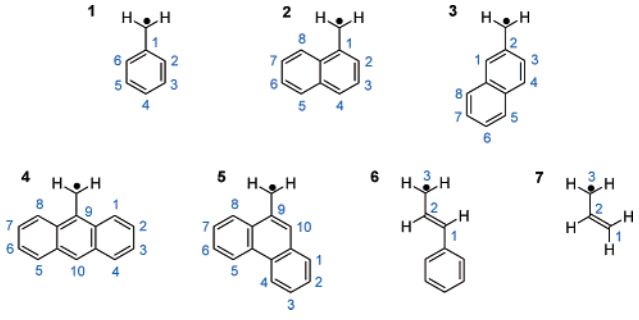

Table 1. Bond Dissociation Energies, Enthalpies, and Free Energies[a]

parameter and theor. level		1H	2H	3H	4H	5H	6H	7H
BDE	B3LYP/6−31G* :=A	94.90	93.82	94.21	88.50	94.28	87.23	92.19
	B3LYP/6−311G**//A	94.12	94.16	94.76	88.94	94.63	87.47	92.60
	QCISD/6−311G**//A	95.34	96.60	96.66	91.73	99.38	89.13	91.62
BDH_0	B3LYP/6−31G*	86.48	85.23	85.77	80.16	85.57	79.01	83.57
	B3LYP/6−311G**//A	85.70	84.38	85.13	79.41	84.74	78.07	82.80
	QCISD/6−311G**//A	86.92	88.00	88.21	83.38	90.67	80.91	83.00
BDH_{298}	B3LYP/6−31G*	87.07	85.96	86.38	80.77	86.37	79.62	84.30
	B3LYP/6−311G**//A	86.28	85.12	85.75	80.02	85.54	78.67	83.53
	QCISD/6−311G**//A	87.50	88.73	88.83	84.00	91.47	81.52	83.73
BDG	B3LYP/6−31G*	79.57	77.69	78.61	72.81	77.84	72.17	76.20
	B3LYP/6−311G**//A	78.79	76.85	77.97	72.06	77.01	71.23	75.43
	QCISD/6−311G**//A	80.01	80.47	81.05	76.03	82.94	74.07	75.63

[a] All energies in kilocalories per mole.

are discussed in the context of "common knowledge" shaped by Hückel molecular orbital (HMO) theory.

Theoretical and Computational Methods

Structures were optimized at the B3LYP/6-31G* level and characterized by vibrational analysis using restricted and unrestricted wavefunctions for **1H**−**7H** and **1**−**7**, respectively.[21] The closed-shell hydrocarbons are C_s-symmetric and, except for toluene, the C_s plane coincides with the molecular plane. Except for **4**, the radicals also are C_s-symmetric and planar, and radicals **1** and **7** are C_{2v}-symmetric. Unexpectedly, we find that radical **4** shows a slight preference for a nonplanar C_s-symmetric structure; that is, its CH_2 group is moved out of the best plane of the anthracene. The structures of all radicals were optimized without symmetry constraints and starting with slightly asymmetric initial guess structures so that the resulting de facto symmetries were established for the minima and confirmed by the analytical computations of the Hessian matrices. Details of the potential energy surface analysis are provided in the Supporting Information, and the data include Cartesian coordinates and molecular models of the optimized structures, total energies E_{tot}, vibrational zero-point energies VZPE, thermal energies TE, and molecular entropies S.

Bond dissociation energies $BDE = \Delta E(R{-}H \rightarrow R\bullet + H\bullet)$, enthalpies $BDH_0 = \Delta(E + VZPE)$ and $BDH_{298} = \Delta(E + TE)$, and free energies $BDG = \Delta(E + TE - 298.15S)$ are summarized in Table 1. These values were first determined with the data obtained at the level of optimization, B3LYP/6-31G* (:= level "A"). More accurate energies were computed with the 6-311G** basis set in two ways: again with the B3LYP method and then also with the quadratic configuration interaction method QCISD. These single-point energy calculations were based on the structures determined at the level B3LYP/6-31G* (:= A), for example, B3LYP/6-311G**//A and QCISD/6-311G**//A, and the BDH and BDG data in Table 1 include the thermal corrections determined at the level of optimization.

Electron and spin densities were computed for all systems at the levels B3LYP/6-311G**//A (:= level "B") and QCISD/6-311G**//A (:= level "C") and for comparison also with extended HMO theory.[22] Electronic structures were examined by natural population analysis[23] and by inspection of surface maps of spin density distributions. Pertinent results are summarized in Table 2, and details are provided in the Supporting Information.

Spin density distributions are illustrated as surface maps in Figure 1 for the prototypical benzyl and allyl radicals and in Figure 2 for radicals **2**−**6**. The generation of such a surface begins with the determination of an isodensity surface of the molecular electron density for a given value of the electron density. We employed the same isodensity surface in all cases, and specifically the one computed at level "B". The value of the spin density is then determined for the entire isosurface, and its distribution is presented via color-coding. Regions shown in blue indicate high α-spin density; those shown in green are relatively spin-free, and regions shown in red show the accumulation of β-spin density.

Calculations were performed with Gaussian 03[24] on the 64-processer SGI Altix system of MU Research Support Computing. Even though the performance of this system is quite astounding, the magnitude of the computational task presented by the present study still posed challenges. The QCISD calculations of the large radicals **4** and **5** required the option "tran=IJAB" so that the integral transformation was possible with the available disk space usage (ca. 1 TB) and, in fact, proceeded with a rather small disk usage (ca. 25 GB). Even then, these radicals were too large to compute the QCI density by the default process. Instead, the value of CONVER had to be reduced such that the convergence on the wavefunction was set to 10^{-6}. Control calculations of the spin density distribution and the natural bond order data of the allyl radical with default and less-restrictive CONVER settings showed that the spin density distribution had converged.

Results and Discussion

Experimental Bond Dissociation Energies. The accurate measurement of the bond dissociation energy of toluene has been difficult. Early on, the bond dissociation energy of toluene in the gas phase was thought to be as low as $\Delta H_{298} = 77.5$ kcal/mol,[25] whereas the modern values are close to 90 kcal/mol. In 1990, Hippler and Troe[26] reported $\Delta H_{298} = 90.4 \pm 1$ and $\Delta H_0 = 88.9 \pm 1$ kcal/mol, and these values were based on the direct measurements of the rate constants of the forward and backward reactions of the equilibrium

Table 2. Spin Density Distributions in Radicals **1**−**7**

parameter	1	2	3	4	5	6	7
				B3LYP/6−311G**			
CH_2	0.68	0.59	0.64	0.40	0.59	0.46	0.62
$C_{ipso}(CH_2)$	−0.14	−0.15	−0.14	−0.14	−0.15	−0.17	−0.20
C_i-CH_2	0.54	0.44	0.50	0.26	0.44	0.29	0.40
C_o-H	0.21	0.30	0.11		0.38	0.50	0.62
C_m-H	−0.10	−0.12	−0.09				
C_p-H	0.23	0.30		0.42			
C_o in CH	0.21	0.31	0.11		0.39	0.52	0.62
C_m in CH	−0.10	−0.12	−0.09				
C_p in CH	0.24	0.31		0.43			
C_o in CR		0.12		0.17	0.06		
C_m in om−CR		−0.07		−0.10	−0.04		
C_m in mp−CR			−0.08		−0.09	−0.10	
C_p in CR			0.13		0.13	0.15	
C_2H_2	0.11	0.18	0.03				
om-$C_2C_4H_4$		0.09		0.16	0.01		
mp-$C_2C_4H_4$			0.15		0.17	0.21	
				QCISD/6−311G**			
CH_2	0.69	0.60	0.65	0.42	0.60	0.46	0.61
$C_{ipso}(CH_2)$	−0.20	−0.22	−0.21	−0.21	−0.22	−0.22	−0.23
C_i-CH_2	0.49	0.38	0.43	0.22	0.38	0.24	0.38
C_o-H	0.26	0.36	0.18		0.45	0.57	0.63
C_m-H	−0.15	−0.19	−0.15				
C_p-H	0.29	0.36		0.48			
C_o in CH	0.26	0.38	0.19		0.47	0.59	0.66
C_m in CH	−0.15	−0.20	−0.16				
C_p in CH	0.30	0.37		0.50			
C_o in CR		0.18		0.24	0.13		
C_m in om−CR		−0.13		−0.17	−0.12		
C_m in mp−CR			−0.15		−0.16	−0.17	
C_p in CR			0.20		0.21	0.19	
C_2H_2	0.11	0.17	0.03				
om−$C_2C_4H_4$		0.09		0.15	0.02		
mp−$C_2C_4H_4$			0.14		0.15	0.19	
				Extended Hückel Theory			
CH_2	0.53	0.41	0.47	0.23	0.41	0.33	0.50
$C_{ipso}(CH_2)$	0.00	0.00	0.00	0.00	0.00	0.00	0.00
C_i-CH_2	0.53	0.41	0.47	0.23	0.41	0.33	0.50
C_o-H	0.15	0.21	0.05		0.29	0.38	0.50
C_m-H	0.00	0.00	0.00				
C_p-H	0.17	0.22		0.29			
C_o in CH	0.15	0.21	0.05		0.29	0.38	0.50
C_m in CH	0.00	0.00	0.00				
C_p in CH	0.17	0.22		0.29			
C_o in CR		0.06		0.09	0.02		
C_m in om−CR		0.00		0.00	0.00		
C_m in mp−CR			0.00		0.00	0.00	
C_p in CR			0.08		0.09	0.09	
C_2H_2	0.15	0.21	0.05				
om−$C_2C_4H_4$		0.16		0.24	0.05		
mp−$C_2C_4H_4$			0.23		0.25	0.29	

$C_6H_5-CH_3 \rightleftarrows C_6H_5-CH_2\bullet + \bullet H$. The value $\Delta H_{298} = 88.5 \pm 1.5$ kcal/mol was given in the 1994 review by Berkowitz et al.,[27] and in 1996, Ellison et al.[28] reported the values $\Delta H_{300} = 89.8 \pm 0.6$ and $\Delta H_0 = 88.1 \pm 0.6$ kcal/mol. These values were derived from the measurement of ΔG_{300} for the gas-phase equilibrium $C_6H_5-CH_3 + CH_3O^- \rightleftarrows C_6H_5-CH_2^- + CH_3OH$ in conjunction with the knowledge of ΔS_{300} for this equilibrium, the gas phase acidity of methanol, the electron affinity of the benzyl radical, and an estimation of the thermal correction ($\Delta H_0 = \Delta H_{300} - 1.6 \pm 0.2$ kcal/mol). With the more recent value for the gas-phase acidity of methanol reported by Ervin and DeTuri in 2002[29] as $\Delta G_{298} = 375.5 \pm 0.6$ kcal/mol and 0.4 kcal/mol higher than the earlier value, the derivation by Ellison et al. results in 0.4 kcal/mol

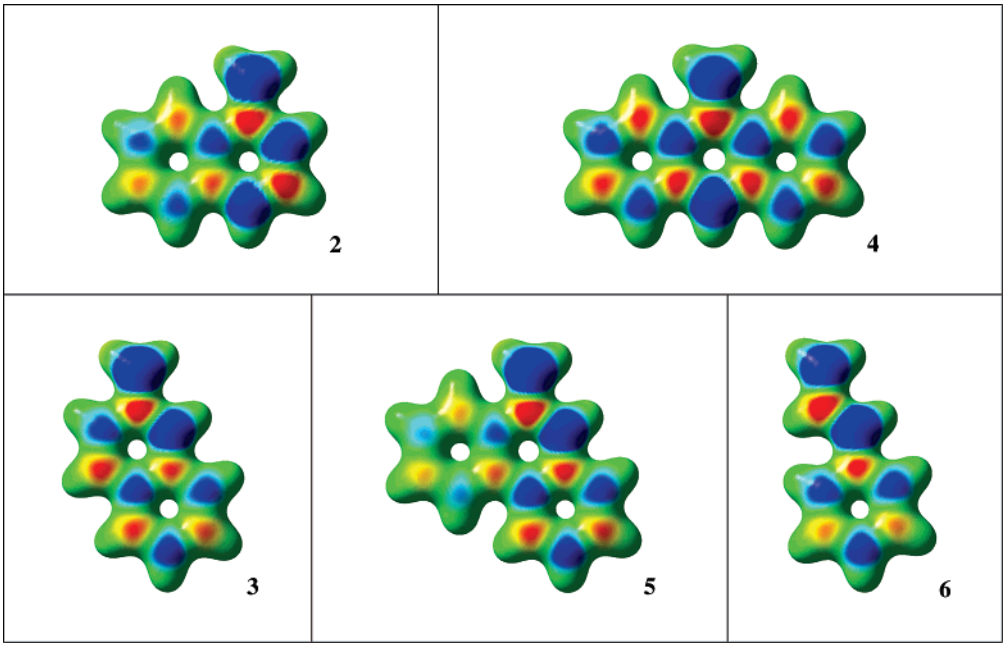

Figure 2. Spin density distributions of benzannulated benzyl radicals **2**−**5** and model **6**. Spin densities are color-coded as in Figure 1 from -4.432×10^{-3} to 4.432×10^{-3} and displayed on isosurfaces of the electron densities (value 0.04).

increases to the values $\Delta H_{300} = 90.2 \pm 0.6$ and $\Delta H_0 = 88.6 \pm 0.6$ kcal/mol. Thus, there exists complete agreement between the measurements of the bond dissociation energy of toluene by the two different approaches.

Benzannulation is thought to provide additional radical stabilization because benzannulation is thought to result in additional electron and spin delocalization as indicated for radical **4** in Chart 1 (**B-1**−**B-4** etc.). Yet, the experimental and theoretical records on benzannulated benzyl radicals are scarce, and this assumption has never been really tested. Finkelshtein's compilation indicates reductions of the bond dissociation energies of 1-methylnaphthalene and 9-methylanthracene by 3.4 and 4.4 kcal/mol for single and double benzannulation, respectively.[30] The bond dissociation energies computed by Bauschlicher and Langhoff at the B3LYP/4-31G level for 1-methylnaphthalene, 1-methylanthracene, and 9-methylanthracene are respectively 0.7, 0.6, and 3.7 kcal/mol lower than for toluene.[31] The suggestion that monoannulation would have but a negligible effect on the benzylic C−H bond dissociation energy was stated without comment in spite of its apparent inconsistency with the available experimental data.[30]

Computed Bond Dissociation Energies. The hydrocarbons all are neutral, nonpolar, and strain-free; basis set effects are expected to be small, and they are; and BDE(A) and BDE(B) data are in excellent agreement. Unless noted otherwise, the bond dissociation enthalpies BDH_{298}(B) are discussed, and the results are as follows: (1) Monoannulation hardly alters the benzylic C−H bond dissociation energy. The BDH_{298}(B) data for **1**−**3** are almost the same, 85.6 ± 0.5 kcal/mol. (2) Dibenzannulation in the anthracene derivative reduces the BDH value by ca. 6 kcal/mol. (3) Dibenzannulation in the phenanthrene derivative results in a BDH value that falls in the range of 85.6 ± 0.5 kcal/mol for **1H**−**3H**.

We first sought corroboration of the finding that BDH_{298}(**2H**) and BDH_{298}(**3H**) are only *slightly* reduced compared to BDH_{298}(**1H**) only to find that the QCISD calculations show that the BDH_{298}(C) values for **2H** and **3H** actually are slightly *higher* than for **1H**. The difference between the BDH_{298} values of **2H** and **3H** relative to **1H** change from −1.2 and −0.5 at level B to +1.2 and +1.3 at level C, respectively, and these changes are about 2 kcal/mol. The respective differences for the larger systems **4H** and **5H** are significantly larger, and they can be as high as about 5 kcal/mol; the difference between the BDH_{298} values of **4H** and **5H** relative to **1H** change from −6.3 and −0.7 at level B to −3.5 and +4.0 at level C, respectively. It is common practice to seek corroboration at higher levels. It also is common practice to seek this corroboration only for small systems and to then argue that the insights gained for the small systems would carry over to larger systems. The latter approach, as common and as accepted as it is, fails quite significantly in the present case!

The theoretical methods employed in the present study give BDH_{298} values for toluene that are about 2−4 kcal/mol lower than the experimental value (vide infra), and the BDH_{298} value derived at the QCISD/6-311G**//B3LYP/6-31G* level is within 2.5 kcal/mol. The bond dissociation energy of propene allows for a second direct comparison with experimental data of high quality. With the modern gas-phase acidity of methanol,[29] the equilibrium measurements by Ellison et al.[28] yield $\Delta H_{300} = 89.2 \pm 0.4$ and $\Delta H_0 = 87.8 \pm 0.4$ kcal/mol, and these values need to be compared to the computed values of $BDH_{298} = 83.7$ and $BDH_0 = 83.0$ kcal/mol (Table 1). The allyl data suggest that the agreement of the computed and experimental benzyl data is perhaps better than one can generally expect at this theoretical level. Nevertheless, to achieve these high levels of agreement between experiment and theory for homolyses is quite

remarkable. For homolyses, the underestimation of the bond dissociation energy is systematic because the UHF treatments of the hydrocarbon radicals are more complete than the RHF treatments of the hydrocarbons. The post-HF methods must correct, and the QCISD method accomplishes this very effectively. Furthermore, the computed thermal correction for the bond dissociation enthalpy of toluene is BDH_{298}(**1H**) − BDH_0(**1H**) = 0.6 kcal/mol (Table 1) and about 1 kcal/mol lower than the thermal correction employed in the experimental studies.[26,28] Part of the underestimation of the bond dissociation enthalpy is thus due to errors in the computed thermal energy correction. Overall, we can be quite confident that the wavefunctions of the radicals are of high quality, and considering that trends in general are less sensitive to the completeness of the theoretical method, it is justified and safe to conclude the following: "Benzannulation per se" does not necessarily lower the benzylic C−H bond dissociation energy. Compared to BDH_{298}(**1H**), the BDH_{298} values of **2H** and **3H** are about 1 kcal/mol higher, the BDH_{298} value of (**5H**) is about 4 kcal/mol higher, and only BDH_{298}(**4H**) is about 3.5 kcal/mol lower.

Spin Density Distributions. Complete sets of q^S data computed for radicals **1**−**7** with DFT and QCI densities are given in Table 2. The spin density distributions computed for benzyl and allyl radicals are illustrated in Figure 1, and the DFT and QCISD results are in qualitative agreement in these cases. However, even the qualitative agreement does not carry over to the benzannulated systems, and the spin density distributions shown for radicals **2**−**6** in Figure 2 were determined at the QCISD level.

The spin delocalization in the allyl radical must result in equal α-spin densities of the CH_2 groups, and the methodological differences only can effect the spin polarization. Spin delocalization in the benzyl radical is much more interesting because there are no such symmetry constraints, and consequently, whether spin delocalization occurs, to what extent spin delocalization occurs, and how spin delocalization effects spin polarization, all of these questions now become dependent on the correlation method. The $q^S(CH_2)$ data computed with the DFT and QCI densities are very similar, but the consequences of the spin delocalization are qualitatively different in significant ways, and we discuss the QCI-derived q^S data.

Spin delocalization in the benzyl radical leaves about two-thirds of one full α spin on the CH_2 group, and the delocalization of one-third of an α spin leads to strong spin polarization: the spin densities on the ortho (≈ 0.26α) and para (≈ 0.29α) CH groups add up to 2−3 times the amount of delocalized total spin, and C_{ipso} (≈ 0.2β) and the meta CH groups (≈ 0.15β) carry β-spin populations.

The illustrations in Figure 2 show in a compelling fashion that spin delocalization onto a benzannulated fragment is *not* the decisive principle and that the spin distribution remaining in the benzyl fragment depends on the type of benzannulation. In **2**, the spin population on the annulated ortho C atom declines and those on the ortho and para CH groups increase, and the resulting spin density closely ressembles that of the homoallyl radical (Chart 3). In **3**, all the spin delocalization occurs to that ortho CH group that is part of a second benzyl

Chart 3. Avoidance of Benzyl Delocalization as Primary Delocalization Mode: Allyl and Homoallyl Systems and Alternative Benzyl Systems as Secondary Modes of Radical Delocations

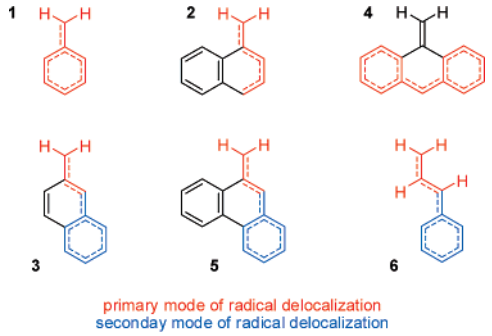

system, and the electronic structure of the 1-phenylallyl radical **6** results. This same electronic structure also characterizes radical **5**, and its second benzannulated ring is essentially spin-free. Spin delocalization occurs via nonannulated bonds in **2**, **3**, and **5**, and this is not possible in **4**. Nonetheless, upon homolysis, massive spin delocalization onto the para CH group does occur [$q^s(C_pH) \approx 0.5\beta$], and the spin populations of the $C_2C_4H_4$ fragments are lower than in **1**. Hence, **4** features the electronic structure of a 2,2′-ethenylene-bridged diphenylmethyl radical. The overall spin on the $C_{ipso}-CH_2$ fragment amounts to a mere 0.2α, and the essence of **4** is its diphenylmethyl radical nature.

Radicals **3**, **5**, and **6** are of special interest because they contain 1-phenylallyl moieties and allow for a direct comparison of the propensity for benzyl-type spin delocalization. The ortho CH group and the C_o atoms of **3**, **5**, and **6** show α-spin populations that are greatly increased as compared to the respective moieties in **1** and **2**, respectively, and well-recognizable "allyl radical spin systems" result. The important point here is the finding that this delocalization of spin density onto the phenyl substituted C atom would allow for benzyl-type delocalization into the "annulated arene" (shown in blue in Chart 3) and that such benzyl-type delocalizaton actually occurs *much less* than in radicals **1** and **4** where benzyl-type delocalization is the only option. The same argument applies to **2** where the para CH group and C_p carry large α-spin populations but benzyl-type delocalization into the "annulated ring" is only modest.

The spin density analysis thus explains the low value for the benzylic C−H bond dissociation energy of **4H**: Homolysis creates the diphenylmethyl radical **4**, whereas radicals **2**, **3**, **5**, and **6**, on the other hand, are homoallyl or phenylallyl systems. There is one-half of an α-spin density on the C_pH group of **4**, that is, the "methyl moiety" of the diphenylmethyl radical (cf. **B-4** in Chart 1). Compared to the benzyl radical itself, the second benzene leads to the additional delocalization of merely 0.1 of an unpaired α spin! This very fact shows that delocalization per se is not the general principle for stabilization it is thought to be—not even when benzyl radical stabilization is the only option. The key insight here is that radical **4** is not stabilized because twice as much spin delocalization occurs as in the benzyl radical itself. Rather, radical **4** can achieve spin delocalization while minimizing

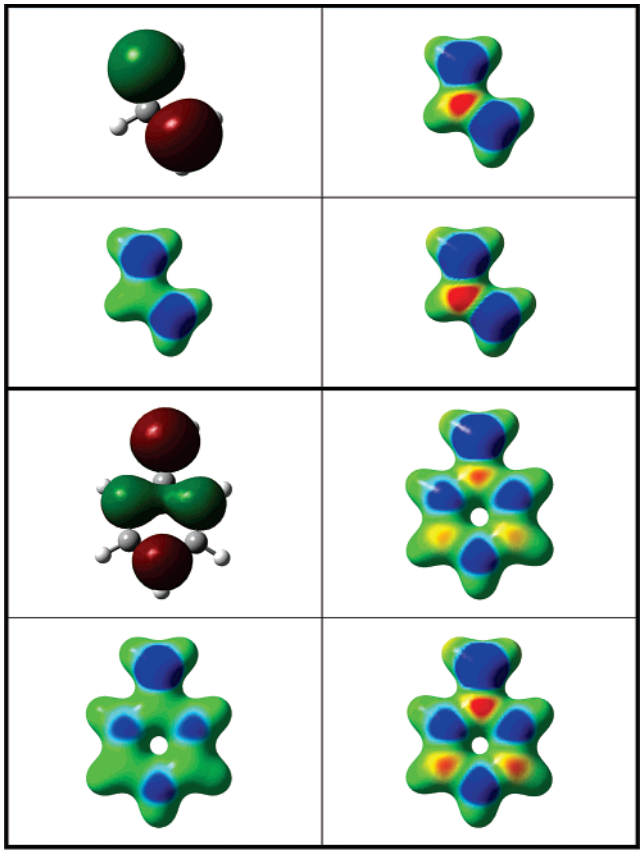

Figure 3. Conceptualization of the spin density distributions in the allyl radical (top) and benzyl radical (bottom). For each radical are shown the HOMO (top, left) and mapped surface plots of the spin densities computed with Hückel theory (bottom, left), density functional theory (top, right), and quadratric CI theory (bottom, right).

the destabilization associated with "spin delocalization onto an aromatic ring."

Spin Delocalization and/or Spin Polarization. The qualitative patterns of the spin delocalizations can be predicted by any linear combination of atomic orbitals molecular orbital (LCAO-MO) theory: from Hückel theory[32−34] and extended Hückel theory[35] to Hartree−Fock theory[36,37] by inspection of the shape of the highest occupied molecular orbital (HOMO) or by spin density analysis.[38,39] Quantitative methods for spin density analysis must account for spin polarization and require electron correlation, that is, the application of post-HF methods in the context of MO theory. On the other hand, spin polarization enters naturally in valence bond (VB) thought culture.[40] The DFT and the QCI methods recover the α-spin distribution pattern suggested by VB resonance theory, but these methods differ greatly in their effectiveness.

In HMO theory, spin density distribution usually is discussed by inspection of the HOMO. To provide for a direct comparison by way of the DFT and QCISD spin-density mapped electron density surfaces of Figures 1 and 2, we computed such surfaces also at the HMO level using extended HMO theory. Figures 3−5 show the results for the prototypical radicals **1** and **7**, the annulated systems, and the diannulated systems, respectively. The HMO spin-density mapped electron density surface for the benzyl radical shown

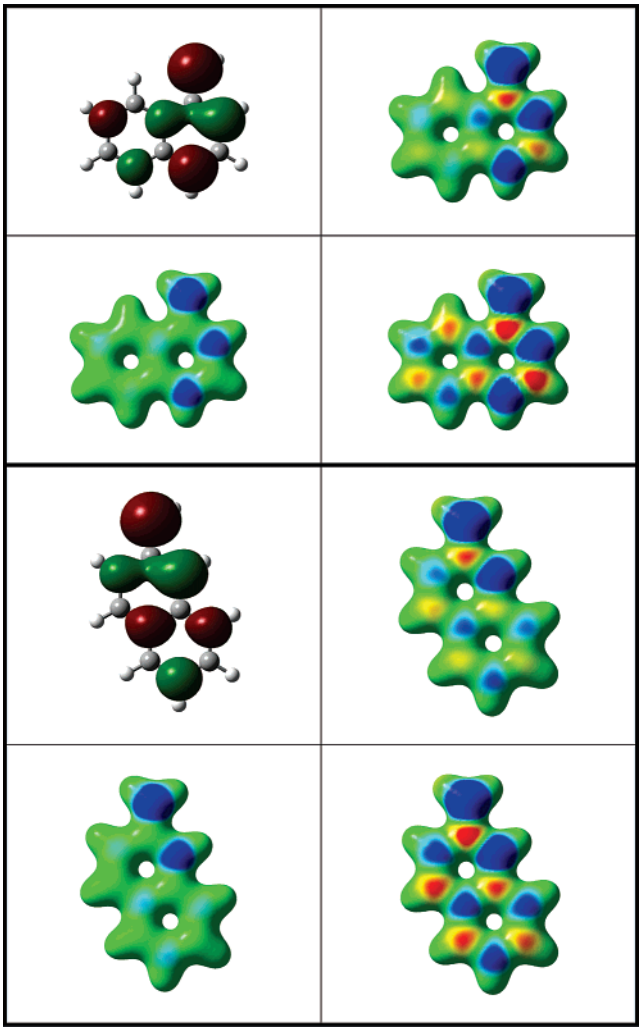

Figure 4. Conceptualization of the spin density distributions of the benzannulated benzyl radicals **2** (top) and **3**. See caption to Figure 3.

in Figure 3 features much less α-spin accumulations on the ortho and para positions as compared to the DFT and QCISD methods; this is the graphical manifestation of the fact that spin delocalization has significant consequences on spin polarization! Many organic chemists might react with disbelief when confronted with the HMO spin-density mapped electron density surfaces for **2**−**6** because there is hardly any spin delocalization into the arenes.

Figures 3−5 show in a compelling fashion that the spin density distributions cannot be understood, not even qualitatively, without consideration of spin polarization. QCISD theory shows significantly more spin polarization and extends over a longer range as compared to the B3LYP method. While molecule-wide spin polarization occurs, there is a tendency to keep the extent of spin delocalization into the annulated arenes *as low as possible*. Spin delocalization into an arene comes at a cost because spin delocalization *requires* spin polarization and thereby causes electronic structures that are less ideal from the perspective of aromaticity.[41]

Conclusion

Chemists use valence bond theory whenever they engage in "electron-pushing", and doing so for radicals creates the

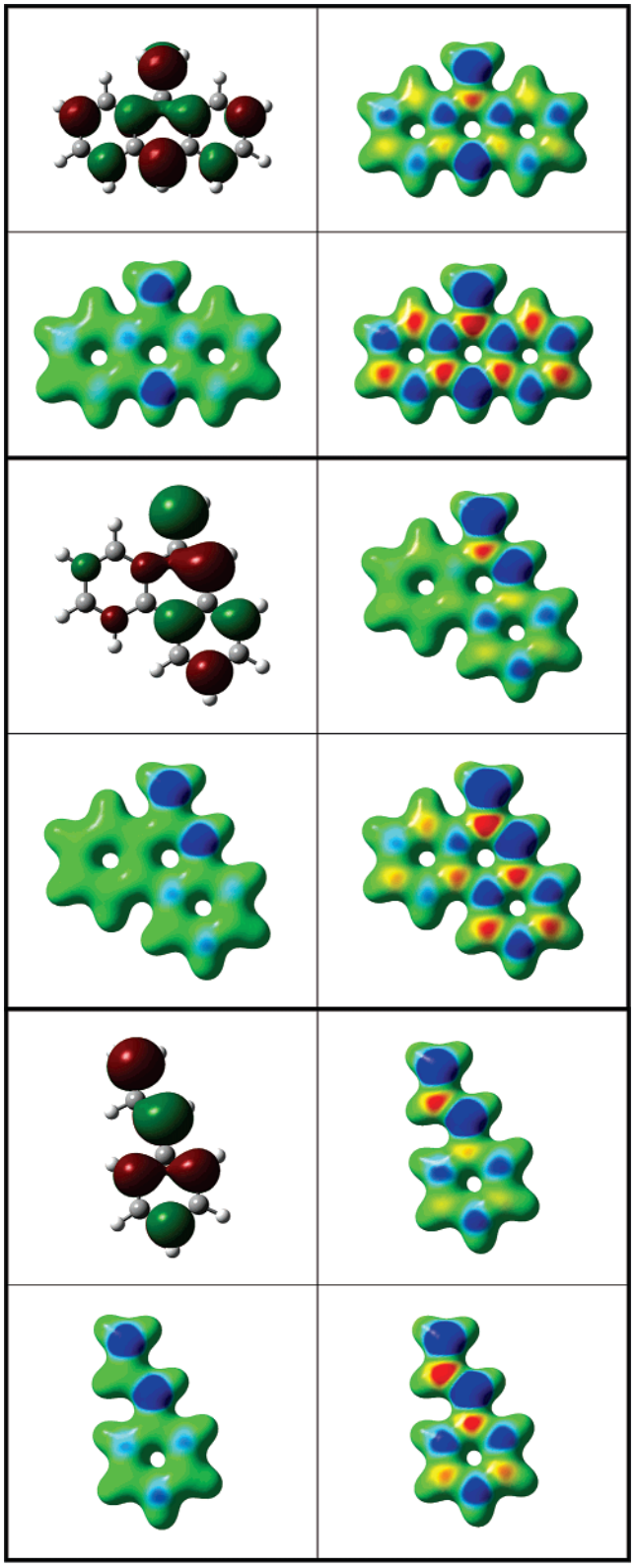

Figure 5. Conceptualization of the spin density distributions of the dibenzannulated benzyl radicals **4** (top) and **5** (center) and of model **6**. See caption to Figure 3.

perception of the possibility of molecule-wide spin delocalization in conjugated systems. On the other hand, whenever chemists employ computational methods, they are likely to use an uncorrelated LCAO-MO method, and doing so creates the perception of limiting spin delocalization over the HOMO region of the molecule. Neither of these viewpoints is satisfactory. At the core of this problem is a general lack of understanding of "spin polarization" outside of the small circle of theorists. Graduate education in chemistry must begin to include at least qualitative discussions of the effects of spin polarization as a fundamental concept for long-distance communication in molecules. It is hoped that the present article contributes to furthering this long-term goal.

As a more immediate result, the present contribution demonstrates the need for experimental measurements of bond dissociation energies of the benzannulated systems. These data are most pertinent in and of themselves and as the key reference for theoretical studies that will advance fundamental conceptions about bonding.

From the theoretical perspective, the present paper highlights significant differences between the wavefunctions computed with the most widely used implementation of density functional theory and the QCISD method. Considering the computational demand of large-molecule calculations with QCI theory, one wonders whether DFT-based methods can be developed that account more fully for spin-polarization with regard to both magnitude and reach.

Acknowledgment. We acknowledge helpful communications with Dr. Paul Wenthold about the bond dissociation energy of toluene. We thank Drs. Gordon Springer, Larry Sanders, and Slava Zagrzewki for their continued advice about hardware and software issues. This work was supported in part by the MU Research Board (RB #2358). We gratefully acknowledge support of MU Research Computing by Federal Earmark NASA Funds for Bioinformatics Consortium Equipment and additional financial support from Dell, SGI, Sun Microsystems, TimeLogic, and Intel.

Supporting Information Available: Details of the potential energy surface analyses (Cartesian coordinates, total energies E_{tot}, thermal energies *TE*, thermal entropies *S*) and details of the electronic structure analyses (atom charges *q*, atom spin populations q^S). This material is available free of charge via the Internet at http://pubs.acs.org.

References

(1) Dust, J. M.; Arnold, D. R. *J. Am. Chem. Soc.* **1983**, *105*, 1221−1227.

(2) Creary, X. *Acc. Chem. Res.* **2006**, *39*, 761−771.

(3) Wen, Z.; Li, Z.; Shang, Z.; Cheng, J.-P. *J. Org. Chem*. **2001**, *66*, 1466−1472.

(4) Adam, W.; Kita, F.; Harrer, H. M.; Nau, W. M.; Zipf, R. *J. Org. Chem.* **1996**, *61*, 7056−7065.

(5) Wu, Y. D.; Wong, C. L.; Chan, K. W.; Ji, G. Z.; Jiang, X. K. *J. Org. Chem*. **1996**, *61*, 746−750.

(6) Bally, T.; Borden, W. T. *Rev. Comput. Chem.* **1999**, *13*, 1−97.

(7) Hehre, W. J.; Radom, L.; Schleyer, P. v.; Pople, J. *Ab Initio Molecular Orbital Theory*; Wiley-Interscience: New York, 1986.

(8) Cramer, C. J. *Essentials of Computational Chemistry: Theories and Models*, 2nd ed.; John Wiley & Sons: New York, 2004.

(9) Lunell, S. *Chem. Phys. Lett.* **1972**, *13*, 93−96.

(10) Pauncz, R. *Fundam. World Quantum Chem.* **2003**, *1*, 155−181.

(11) Schlegel, H. B. *J. Phys. Chem.* **1988**, *92*, 3075−3078.

(12) Chen, W.; Schlegel, H. B. *J. Chem. Phys.* **1994**, *101*, 5957−5968.

(13) Glaser, R.; Chen, G. S.; Grützmacher, H. *J. Comput. Chem.* **1997**, *18*, 1023−1035.

(14) Pople, J. A. *Rev. Mod. Phys.* **1999**, *71*, 1267−1274.

(15) Wilson, S. *Handb. Mol. Phys. Quantum Chem. 2003* **2003**, *2*, 314−373.

(16) He, Z.; Kraka, E.; Cremer, D. *Int. J. Quantum Chem.* **1996**, *57*, 157−172.

(17) Koch, W.; Holthausen, M. C. *A Chemist's Guide to Density Functional Theory*, 2nd ed.; Wiley-VCH: Weinheim, Germany, 2001.

(18) Parr, R. G; Weitao, Y. *Density-Functional Theory of Atoms and Molecules*; Oxford University Press: Oxford, U. K., 1994; International Series of Monographs on Chemistry.

(19) Wittbrodt, J. M.; Schlegel, H. B. *J. Chem. Phys.* **1996**, *105*, 6574−6577.

(20) Noodleman, L.; Lovell, T.; Han, W.-G.; Li, J.; Himo, F. *Chem. Rev.* **2004**, *104*, 459−508.

(21) ReePeng, C.; Ayala, P.; Schlegel, H. B.; Frisch, M. J. *J. Comput. Chem.* **1996**, *17*, 49−56.

(22) Hoffmann, R. *J. Chem. Phys.* **1964**, *40*, 2474−2478.

(23) Reed, A. E.; Weinstock, R. B.; Weinhold, F. *J. Chem. Phys.* **1985**, *83*, 735−746.

(24) Frisch, M. J.; Trucks, G. W.; Schlegel, H. B.; Scuseria, G. E.; Robb, M. A.; Cheeseman, J. R.; Montgomery, J. A., Jr.; Vreven, T.; Kudin, K. N.; Burant, J. C.; Millam, J. M.; Iyengar, S. S.; Tomasi, J.; Barone, V.; Mennucci, B.; Cossi, M.; Scalmani, G.; Rega, N.; Petersson, G. A.; Nakatsuji, H.; Hada, M.; Ehara, M.; Toyota, K.; Fukuda, R.; Hasegawa, J.; Ishida, M.; Nakajima, T.; Honda, Y.; Kitao, O.; Nakai, H.; Klene, M.; Li, X.; Knox, J. E.; Hratchian, H. P.; Cross, J. B.; Bakken, V.; Adamo, C.; Jaramillo, J.; Gomperts, R.; Stratmann, R. E.; Yazyev, O.; Austin, A. J.; Cammi, R.; Pomelli, C.; Ochterski, J. W.; Ayala, P. Y.; Morokuma, K.; Voth, G. A.; Salvador, P.; Dannenberg, J. J.; Zakrzewski, V. G.; Dapprich, S.; Daniels, A. D.; Strain, M. C.; Farkas, O.; Malick, D. K.; Rabuck, A. D.; Raghavachari, K.; Foresman, J. B.; Ortiz, J. V.; Cui, Q.; Baboul, A. G.; Clifford, S.; Cioslowski, J.; Stefanov, B. B.; Liu, G.; Liashenko, A.; Piskorz, P.; Komaromi, I.; Martin, R. L.; Fox, D. J.; Keith, T.; Al-Laham, M. A.; Peng, C. Y.; Nanayakkara, A.; Challacombe, M.; Gill, P. M. W.; Johnson, B.; Chen, W.; Wong, M. W.; Gonzalez, C.; Pople, J. A. *Gaussian 03*, revision D.01; Gaussian, Inc.: Wallingford, CT, 2004.

(25) Szwarc, M. *J. Chem. Phys.* **1948**, *16*, 128−136.

(26) Hippler, H.; Troe, J. *J. Phys. Chem.* **1990**, *94*, 3803−3806.

(27) Berkowitz, J.; Ellison, G. B.; Gutman, D. *J. Phys. Chem.* **1994**, *98*, 2744−2765.

(28) Ellison, G. B.; Davico, G. E.; Bierbaum, V. M.; DePuy, C. H. *Int. J. Mass Spectrom. Ion Processes* **1996**, *156*, 109−131.

(29) Ervin, K. M.; DeTuri, V. F. *J. Phys. Chem. A* **2002**, *106*, 9947−9956.

(30) Finkelshtein, E. I. *J. Phys. Org. Chem.* **2001**, *14*, 543−550.

(31) Bauschlicher, C. W.; Langhoff, S. R. *Mol. Phys.* **1999**, *96*, 471−476.

(32) Streitwieser, A. *Molecular Orbital Theory for Organic Chemists*; John Wiley & Sons: New York, 1961; p 392ff.

(33) Carsky, P.; Zahradnik, R. *J. Phys. Chem*. **1970**, *74*, 1249−1254.

(34) Nowakowski, J. *Theor. Chim. Acta* **1970**, *18*, 133−142.

(35) Hoffmann, R.; Bissell, R.; Farnum, D. G. *J. Phys. Chem.* **1969**, *73*, 1789−1800.

(36) Gey, E.; Hennig, H.; Stoesser, R. *Z. Phys. Chem. (Liepzig)* **1974**, *255*, 395−400.

(37) Klimo, V.; Tino, J. *Int. J. Quantum Chem.* **1976**, *10*, 761−769.

(38) Glaser, R.; Choy, G. S.-C. *J. Phys. Chem.* **1993**, *97*, 3188−3198.

(39) Glaser, R.; Choy, G. S.-C. *J. Phys. Chem.* **1994**, *98*, 11379−11393.

(40) Wu, W.; Zhong, S.; Shaik, S. *Chem. Phys. Lett.* **1998**, *292*, 7−14.

(41) Shurki, A.; Hiberty, P. C.; Dijkstra, F.; Shaik, S. *J. Phys. Org. Chem*. **2003**, *16*, 731−745.

CT700051J